Numerical Investigation on Hypersonic Flat-Plate Boundary Layer Transition Subjected to Bi-frequency Synthetic Jet

Xinyi Liu , Zhenbing Luo * , Qiang Liu * , Pan Cheng , Yan Zhou

Posted Date: 2 June 2023

doi: 10.20944/preprints202306.0155.v1

Keywords: hypersonic boundary layer transition; transition delay; bi-frequency synthetic jet; flow control; linear stability theory

 doi:10.20944/preprints202306.0155.v1

Article

Numerical Investigation on Hypersonic Flat-Plate Boundary Layer Transition Subjected to Bi-Frequency Synthetic Jet

Xinyi Liu, Zhenbing Luo *, Qiang Liu *, Pan Cheng and Yan Zhou

College of Aerospace Science and Engineering, National University of Defense Technology, Changsha, 410073, China

* Correspondence: luozhenbing@163.com (Z.L.); liuqiang12@nudt.edu.cn (Q.L.)

Abstract: Transition delaying is of great importance for the drag and heat flux reduction of hypersonic flight vehicles. The first mode within low frequency and the second mode within high frequency exist simultaneously during the transition of hypersonic boundary layer. This paper proposes a novel bi-frequency synthetic jet to suppress low- and high-frequency disturbances at the same time. Orthogonal table and variance analysis are used to compare the control effects of jet with different frequencies, amplitudes and positions. Linear stability analysis results show that, low frequency synthetic jet can suppress the first mode when it is arranged upstream of synchronization point, while the second mode control effect is relatively weak. The higher the high frequency is, the stronger the suppression effect is on the first mode. For the second mode, the suppression effect is only at f_2=89.09kHz. The larger the amplitude, the weaker the promoting effect for the first mode and the second mode, and the more obvious the suppressing effect. For the cases with synthetic jet downstream of synchronization point, all levels of the three parameters promote the unstable mode. In terms of the growth rate with the spanwise wave number, the control effect of the same factor and level under different spanwise wave number is different. In order to obtain the optimal control effect on transition, the three factors and the arrangement position of the synthetic jet should be selected as follows: the position is arranged in the upstream, with f_1 = 3.56kHz, f_2 = 89.9kHz, a =0.009, so that the maximum growth rate of the first mode is reduced by 9.06% and that of the second mode is reduced by 1.28% compared with the uncontrolled state. And it weakens the twin lattice structure of pressure pulsation, thus improves the stability of the flow.

Keywords: hypersonic boundary layer transition; transition delay; bi-frequency synthetic jet; flow control; linear stability theory

1. Introduction

In the design of hypersonic vehicle, boundary layer transition is an important research direction. This is because after the boundary layer transition, the friction drag and heat flux of turbulent boundary layer are usually 3-5 times than that of the laminar ones [1]. Through the delaying of transition, the friction drag and heat flux of boundary layer will be greatly reduced, which leads to the weight reduction of thermal protection system and improvement of its flight range and load.

It is generally believed that transition is caused by the eventual instability of disturbance evolution over time and space. The process of transition is different depending on the initial disturbance [2,3]. For the different stages of transition, the relevant theories are linear stability theory, nonlinear theory, receptivity problem [4–6], etc. For hypersonic boundary layer transition, in addition to the first mode corresponding to incompressible flow, the second mode usually plays a dominant role [7].

Up to now, factors that affecting the hypersonic boundary layer transition include pressure gradient, surface shape, roughness, wall temperature, total pressure and compressibility, et al. [8–10].

 doi:10.20944/preprints202306.0155.v1

Transition delaying control methods are usually divided into passive ones and active ones. The former does not require external energy and does not increase energy consumption, while the latter changes the flow field through active energy input, which is more efficient than the passive one. Common passive transition control has vortex generator [11,12], roughness [13–17], wavy wall [17], porous coatings [18–20]. The active control methods of transition include gas injection [21–23], wall normal jet [24–26], wall heating/cooling [27,28], etc.

In recent years, the active flow control based on synthetic jets has attracted more attention. It has the advantages of being adjustable and controllable, escaping the shortcomings of passive control. The synthetic jet with frequency modulation can produce two peaks of low frequency and high frequency, namely bi-frequency synthetic jet. This paper attempts to control the first mode with low frequency part and the second mode with high frequency part of hypersonic boundary layer based on proposed bi-frequency synthetic jet.

2. Simulation Model

2.1. Freestream Conditions and Numerical Settings

The parameters of the incoming flow in this paper are consistent with the operating parameters of FD-07 wind tunnel in China Academy of Aerospace Aerodynamics. The Mach number of the incoming flow is 6, the temperature is 54.9K, and the unit Reynolds number is 1.0×107/m. The adiabatic wall conditions are used to simulate the boundary layer of Ma 6 plate. The model is a sharp plate with a length of 200mm, as shown in Figure 1. Unsteady blowing and suction disturbance is applied at x=(10mm,15mm). The disturbance form is as follows:

$$q_w = \varepsilon \sin(2\pi \frac{x - x_1}{x - x_2}) \sin(2\pi ft)$$

where, the amplitude ε is 0.0001 and the frequency f is 142.54kHz. That is, a blow and suction disturbance with a fixed frequency is added upstream of the flat-plate.

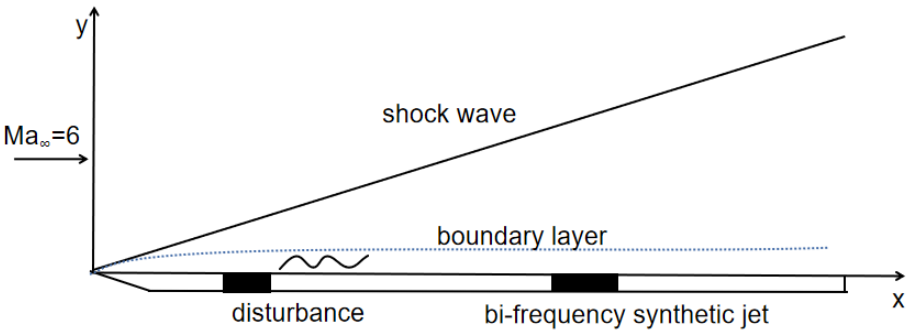

Figure 1. Schematic model of flat-plate with disturbance and control.

The simulation is conducted using the OpenCFD direct numerical simulation codes develop by Li [29]. The codes use finite volume method for discretization, fifth-order WENO scheme to solve inviscid term, sixth-order central difference scheme to solve viscous term, and AUSM to decompose vector flux. The implicit time step is used to solve the undisturbed laminar boundary layer at first. Then, the disturbance is introduced. The implicit double time step method is adopted at first, and then the third order Runge-Kutta method is used to solve the three flows to obtain the stable solution with sufficient time accuracy. A grid of 2420×401 was used, and the grid near the wall was encrypted. The accuracy of the code and the corresponding mesh and boundary layer velocity profiles have been verified by our team [30].

The bi-frequency synthetic jet can be expressed as follows:

$$v_j = a_1 \sin(2\pi f_1 t) + a_2 \sin(2\pi f_2 t)$$

 doi:10.20944/preprints202306.0155.v1

The low frequency is f_1, the high frequency is f_2, and the amplitude is a_1, a_2. f_1 and f_2 are dimensionless frequencies, and the dimensional frequencies is multiplied by 890.89kHz. a_1 and a_2 are the dimensionless amplitudes corresponding to low frequency and high frequency respectively, a_1 and a_2<0.01, if too large, the nonlinearity is obvious and LST cannot be used.

2.2. Orthogonal Experimental Design

Orthogonal experimental design is a fast experimental design method to study the level of multiple factors. It selects representative test combinations from all the tests according to the orthogonality principle of "uniform dispersion, neat and comparable", so that more valuable information can be obtained in a short time by using fewer test times. Multi factor variance analysis is used to study whether a dependent variable is affected by multiple factors. It tests whether there are significant differences between different combinations of multiple factor value levels. One-way analysis of variance (ANOVA) tests the difference of the dependent variable affected by different levels of an independent factor.

The orthogonal table L25(5^3) was used in this experiment. The total number of trials was 25, and 3 factors were tested, each factor tested 5 levels. Without orthogonal tables, 5^3=125 trials would be required to test all combinations of 3 factor with 5 levels, but it only takes 25 times with orthogonal tables. The three factors shown in the table below are the low frequency f_1, the high frequency f_2 and the amplitude a_1=a_2=a. The test level and orthogonal table are shown in Tables 1 and 2.

Table 1. Test level.

Level	*f1*	*f2*	*a*
1	0.004/3.56 kHz	0.04/35.63 kHz	0.001
2	0.008/7.12 kHz	0.06/53.45 kHz	0.003
3	0.012/10.69 kHz	0.08/71.27 kHz	0.005
4	0.016/14.25 kHz	0.10/89.09 kHz	0.007
5	0.020/17.82 kHz	0.12/106.91kHz	0.009

Table 2. Orthogonal table.

Case	f_1	*f2*	*a*
1	0.004/3.56 kHz	0.04/35.63 kHz	0.001
2	0.004/3.56 kHz	0.06/53.45 kHz	0.007
3	0.004/3.56 kHz	0.08/71.27 kHz	0.003
4	0.004/3.56 kHz	0.10/89.09 kHz	0.009
5	0.004/3.56 kHz	0.12/106.91 kHz	0.005
6	0.008/7.12 kHz	0.04/35.63 kHz	0.007
7	0.008/7.13 kHz	0.06/53.45 kHz	0.003
8	0.008/7.14 kHz	0.08/71.27 kHz	0.009
9	0.008/7.14 kHz	0.10/89.09 kHz	0.005
10	0.008/7.14 kHz	0.12/106.91 kHz	0.001
11	0.012/10.69 kHz	0.04/35.63 kHz	0.003
12	0.012/10.69 kHz	0.06/53.45 kHz	0.009
13	0.012/10.69 kHz	0.08/71.27 kHz	0.005
14	0.012/10.69 kHz	0.10/89.09 kHz	0.001
15	0.012/10.69 kHz	0.12/106.91 kHz	0.007

 doi:10.20944/preprints202306.0155.v1

16	0.016/14.25 kHz	0.04/35.63 kHz	0.009
17	0.016/14.25 kHz	0.06/53.45 kHz	0.005
18	0.016/14.25 kHz	0.08/71.27 kHz	0.001
19	0.016/14.25 kHz	0.10/89.09 kHz	0.007
20	0.016/14.25 kHz	0.12/106.91 kHz	0.003
21	0.020/17.82 kHz	0.04/35.63 kHz	0.005
22	0.020/17.82 kHz	0.06/53.45 kHz	0.001
23	0.020/17.82 kHz	0.08/71.27 kHz	0.007
24	0.020/17.82 kHz	0.10/89.09 kHz	0.003
25	0.020/17.82 kHz	0.12/106.91 kHz	0.009

According to the different positions of synthetic jet (upstream: 110-120mm, denoted by USJ; downstream: 150-160mm, denoted by DSJ, with synchronization point in x=134.4mm), two orthogonal tests were carried out respectively, and the parameters of the orthogonal table of the two tests were the same, only the position was different. In addition, it is also necessary to calculate the case under the uncontrolled case.

Conventional methods of studying the effect of a factor by fixing the level of other factors and changing only the level of the factor under study are susceptible to the fixed levels of other factors. However, in the one-way analysis of variance, due to the uniformity and tidiness of the test cases in the orthogonal table, there are more test cases at the same level of the factors under study, including all the levels of other factors, so the average value can eliminate the influence of other factors. For example, if the influence of f_1=3.56kHz is needed to be studied, the first to fifth test cases where f_1=3.56kHz in the orthogonal table, corresponding f_2=35.63kHz to 106.91kHz, a=0.001 to 0.009, uniformly cover all levels of f_2 and a. Take the average value of the test results of cases 1 to 5 to get the influence result of f_1=3.56kHz, so as to avoid the influence of the value of f_2 and a.

2.3. Linear Stability Theory

Linear stability theory is a systematic theory for the study of flow transition. The parallel flow and small disturbance hypothesis are used to study the evolution of small perturbation waves in time and space. The disturbance wave is usually written in the form of wave function:

$$q'(x,y,z,t) = \hat{q}(x,y,z,t)\exp[i(\alpha x + \beta z - \omega t)]$$

where α and β are the wave numbers in the flow direction and spanwise direction, respectively, and ω is the frequency. In the spatial mode, the imaginary part of the flow direction wave number αi represents the growth or attenuation of the disturbance, and less than 0 represents the growth. For the convenience of expression, this paper uses -αi to represent the growth rate, and -α_i>0 represents perturbation growth.

To calculate the disturbance, the flow field needs to be decomposed into the sum of average flow and disturbance:

$$q(x,y,z,t) = \bar{q}(x,y,z,t) + q'(x,y,z,t)$$

The parallel flow hypothesis is introduced, which holds that the change of the variable in the flow direction is small and negligible, i.e.,

$$\bar{\rho} = \bar{u} = \bar{T} = f(y)$$

$$\bar{v} = \bar{u} = 0$$

 doi:10.20944/preprints202306.0155.v1

Putting the disturbance and hypothesis into the governing equation, and simplify to get the linear perturbation equation, namely the O-S equation, whose numerical solution is called T-S wave, solving the O-S equation and analyzing the solution is called linear stability analysis.

In this paper, after the linear stability analysis of the experimental cases arranged in the upstream and downstream and the uncontrolled case, the relationship between the unstable mode growth $-\alpha_i$ rate of each case relative to the frequency ω_r and the spanwise wave number β_r was obtained, and the results were tested by multi-factor and one-way ANOVA, and the significant difference relationship between the low frequency f_1, the high frequency f_2 and the amplitude a was obtained.

3. Variation of Growth Rate with Frequency

Figure 2 shows the growth rate $-\alpha i$ as a function of the dimensionless frequency ωr in the uncontrolled case. It is worth noting that the dimensional frequency is expressed in $\omega r \times 141.79$kHz. Two peaks can be seen in the figure, where the first mode (about 63.8kHz) with a maximum growth rate of 0.00276, and the second mode (about 119.10kHz) with a maximum growth rate of 0.02108. It can be seen that the second mode is the dominant unstable mode in the hypersonic boundary layer.

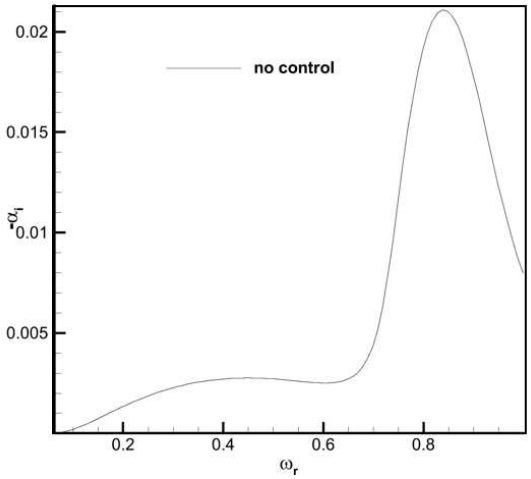

Figure 2. Uncontrolled growth rate as a function of frequency.

3.1. Results of Synthetic Jet Arranged Upstream of Synchronization Point

The maximum growth rate of the first mode and the second mode of each test case is shown in the second and third columns of Table 3, with synthetic jet is arranged upstream. The fourth and fifth columns are the percentages of promotion or suppression of the first and second modes relative to the uncontrolled case. Positive values represent promotion and negative values represent suppression. It can be seen that some test cases promote both modes, some suppress both modes, and some promote the second mode while suppress the first mode.

Table 3. Test results of each case of USJ.

	mode-1	mode-2	mode-1*	mode-2*
1	0.00286	0.02123	3.62%	0.71%
2	0.00286	0.02113	3.62%	0.24%
3	0.00276	0.02118	0.00%	0.47%
4	0.00251	0.02081	- 9.06%	- 1.28%
5	0.00264	0.02125	- 4.35%	0.81%
6	0.00286	0.02126	3.62%	0.85%
7	0.00281	0.02124	1.81%	0.76%

Preprints.org (www.preprints.org) | NOT PEER-REVIEWED | Posted: 2 June 2023 doi:10.20944/preprints202306.0155.v1

8	0.00257	0.02108	- 6.88%	0.00%
9	0.00262	0.02096	- 5.07%	- 0.57%
10	0.00278	0.02119	0.72%	0.52%
11	0.00283	0.02122	2.54%	0.66%
12	0.00286	0.02128	3.62%	0.95%
13	0.00269	0.02116	- 2.54%	0.38%
14	0.00278	0.02115	0.72%	0.33%
15	0.00256	0.0213	- 7.25%	1.04%
16	0.00294	0.02136	6.52%	1.33%
17	0.00284	0.02126	2.90%	0.85%
18	0.0028	0.02119	1.45%	0.52%
19	0.00261	0.02096	- 5.43%	- 0.57%
20	0.00274	0.02129	- 0.72%	1.00%
21	0.00288	0.02126	4.35%	0.85%
22	0.00282	0.02121	2.17%	0.62%
23	0.00268	0.02125	- 2.90%	0.81%
24	0.00271	0.02107	- 1.81%	- 0.05%
25	0.00244	0.02119	- 11.59%	0.52%

Case 16 has the most obvious promotion effect on the first and second modes, with 6.52% and 1.33%, respectively. Case 4 showed the strongest suppressing effects on both first and second mode, which were -9.06% and -1.28%, respectively. The 15th case suppresses the first mode by -7.25%, but promotes the second mode by 1.04%, as shown in Figure 3.

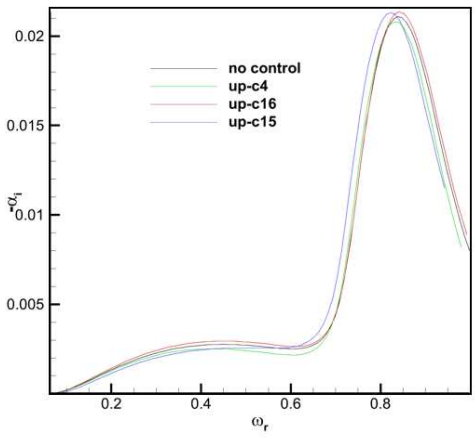

Figure 3. Growth rate varies with frequency in cases 4, 15 and 16 of USJ.

The multi-factor variance analysis of the control effect of the synthetic jet arranged in the upstream on first mode shows that *f2* has a significant difference relation to first mode, while *f1* and a have a small difference relation to first mode, as shown in Table 4.

Table 4. Multivariate ANOVA results of the first mode of the USJ.

Source of variance	Sum of squares	df	Mean square	*F*	*p*
Intercept	0.002	1	0.002	1.975	0.198

Preprints.org (www.preprints.org) | NOT PEER-REVIEWED | Posted: 2 June 2023 doi:10.20944/preprints202306.0155.v1

Source of variance	Sum of squares	df	Mean square	*F*	*p*
f_1	0.002	4	0.001	0.736	0.593
f_2	0.033	4	0.008	10.110	0.003
a	0.008	4	0.002	2.441	0.132
Residual	0.006	12	0.001		

The variance analysis of the control effect of the jet arranged in the upstream on the second mode shows that *f2* has a significant difference relation to the second mode, while *f1* and a have a small difference relation to the second mode, as shown in Table 5. The small difference produced by *f1* and a does not mean that they have poor influence on transition control, but mainly reflects that the two are close within their respective 5 levels, and the level with large difference is needed for further test. In this paper, one-way analysis of variance is still carried out for the three factors including *f1* and a respectively, with the purpose of finding the influence rule of the three factors on the control effect, and the level that can produce the best control effect can be selected after finding the rule.

Table 5. Multivariate ANOVA results of the second mode of the USJ.

Source of variance	Sum of squares	df	Mean square	*F*	*p*
Intercept	0.002	1	0.002	1.975	0.198
f_1	0.002	4	0.001	0.736	0.593
f_2	0.033	4	0.008	10.110	0.003
a	0.008	4	0.002	2.441	0.132
Residual	0.006	12	0.001		

3.1.1. Effects of Low Frequency Control

One-way ANOVA is performed for the first mode growth rates as the frequency changes, which are controlled by the low frequency of USJ, as shown in Figure 4. It can be seen that when f_1=14.25kHz, the growth rate of the first mode is greater than that of the uncontrolled case, and the flow is obviously unstable, while f_1=3.56kHz, 7.12kHz, 10.69kHz, 17.82kHz all play a suppressing role. When f_1=17.82kHz, the suppression effect is the best.

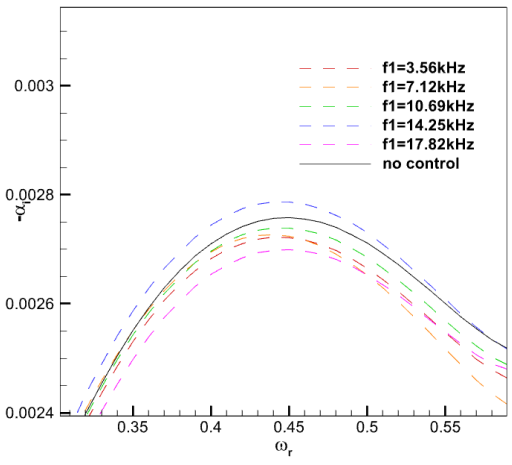

Figure 4. The first mode growth rate varies with frequency, controlled by the low frequency of USJ.

Preprints.org (www.preprints.org) | NOT PEER-REVIEWED | Posted: 2 June 2023 doi:10.20944/preprints202306.0155.v1

The percentage of difference between the maximum growth rate of the first mode and the uncontrolled case is used to make a line plot with the low frequency level, as shown in Figure 5. It can be seen that f_1 shows a suppressing effect when the frequency is low, and the growth rate gradually increases with the increase of f_1, reaching a peak value at f_1=14.25kHz and showing a promoting effect. However, when f_1=17.82kHz, the growth rate drops sharply and turns into a suppressing effect, reaching -2.17%.

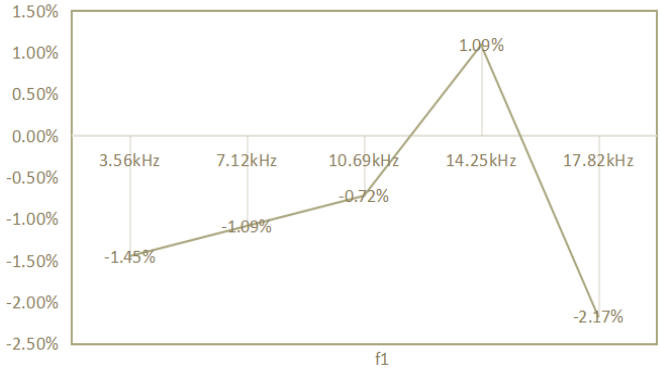

Figure 5. Influence of low frequency of USJ on first mode maximum growth rate.

One-way ANOVA is performed for the second mode growth rates as the frequency changes, which are controlled by the low frequency of USJ, as shown in Figure 6. It can be seen that when f_1=3.56kHz, 7.12kHz, 10.69kHz, 14.25kHz, the growth rate of the second mode is greater than that of the uncontrolled case, and the flow is unstable, while when f_1=17.82kHz, the transition is suppressed.

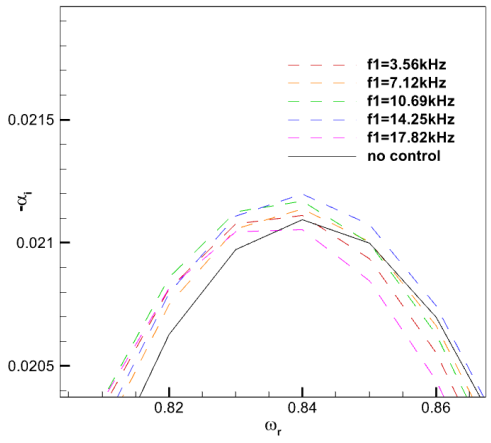

Figure 6. The second mode growth rate varies with frequency, controlled by the low frequency of USJ.

The percentage of difference between the maximum growth rate of the second mode and the uncontrolled case is used to make a line plot with the low frequency level, as shown in Figure 7. It can be seen that the growth rate gradually increases with the increase of f_1, showing a boosting effect and reaching a peak at f_1=14.25kHz, but the growth rate drops sharply when f_1=17.82kHz and turns into a suppressive effect, but the effect is small, only -0.19%. The control effect of low frequency f_1 on the second mode is very small.

To sum up, if the suppression effect is to be achieved on the first and second modes, f_1 should be set at 17.82kHz.

Preprints.org (www.preprints.org) | NOT PEER-REVIEWED | Posted: 2 June 2023 doi:10.20944/preprints202306.0155.v1

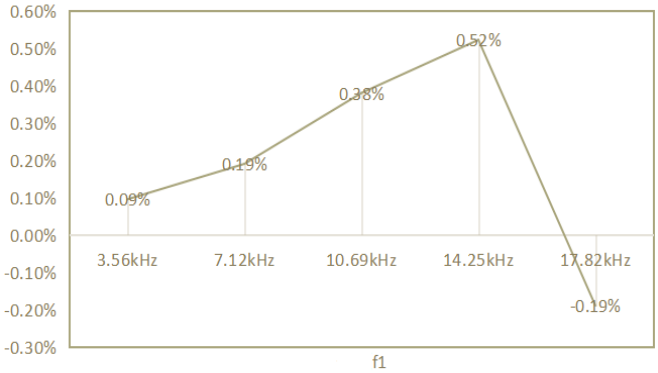

Figure 7. Effect of low frequency of USJ on second mode maximum growth rate.

3.1.2. Effects of High Frequency Control

One-way ANOVA is performed for the first mode growth rates as the frequency changes, which are controlled by the high frequency of USJ, as shown in Figure 8. It can be seen that when f_2=35.63kHz and 53.45kHz, the growth rate of the first mode is greater than that of the uncontrolled case, which plays a role in promoting transition, while when f_2=71.27kHz, 89.09kHz and 106.91kHz, it plays a suppressing role. When f_2=106.91kHz, the suppression effect is the best, and the frequency corresponding to the maximum growth rate of the first mode increases slightly compared with other levels and the uncontrolled case.

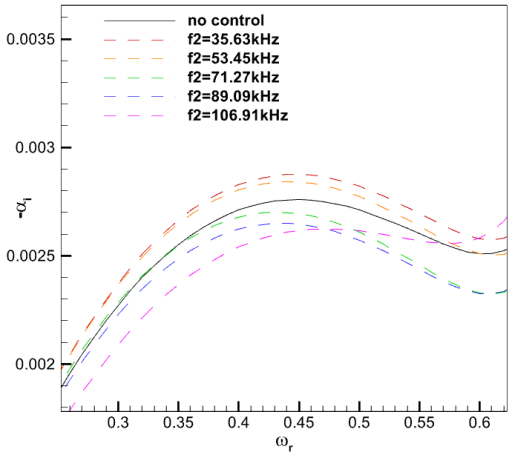

Figure 8. The first mode growth rate varies with frequency, controlled by the high frequency of USJ.

The percentage of difference between the maximum growth rate of the first mode and the uncontrolled case is used to make a line plot with the high frequency level, as shown in Figure 9. It can be seen that with the increase of f_2, the control effect on transition gradually changes from promotion to suppression, and the higher the frequency, the better the suppression effect is, and when f_2=106.91kHz, it reaches -5.07%. Compared with low frequency, the control effect of high frequency f_2 is more obvious.

Preprints.org (www.preprints.org) | NOT PEER-REVIEWED | Posted: 2 June 2023 doi:10.20944/preprints202306.0155.v1

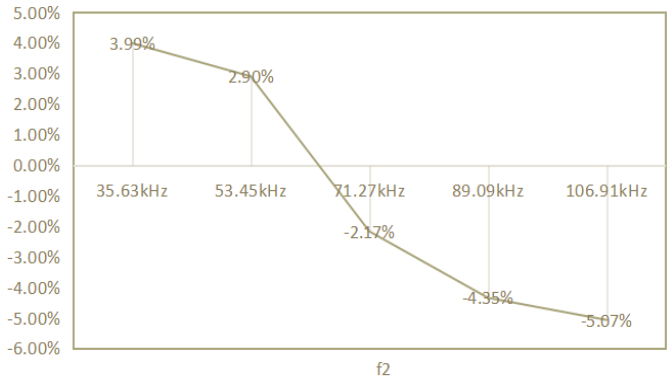

Figure 9. Effect of high frequency of USJ on first mode maximum growth rate.

One-way ANOVA is performed for the second mode growth rates as the frequency changes, which are controlled by the high frequency of USJ, as shown in Figure 10. It can be seen that when f_2=35.63kHz, 53.45kHz, 71.27kHz and 106.91kHz, the second mode growth rate is greater than that of the uncontrolled case, which promotes transition, while when f_2=89.09kHz, it suppresses transition. When f_2=106.91kHz, the frequency corresponding to the maximum growth rate of the second mode is slightly reduced compared with other levels and the uncontrolled case.

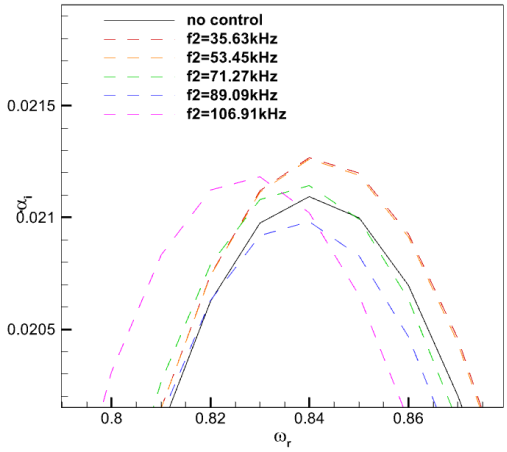

Figure 10. The second mode growth rate varies with frequency, controlled by the high frequency of USJ.

The percentage of difference between the maximum growth rate of the second mode and the uncontrolled case is used to make a line plot with the high frequency level, as shown in Figure 11. It can be seen that with the increase of f_2, the promotion effect on transition gradually decreases, and turns to suppression when f_2=89.09kHz with the suppression effect is -0.52%. Compared with low frequency f_1, the control effect of high frequency f_2 is more obvious.

To sum up, f_2 should be set at 89.09kHz in order to achieve suppression effect on the first and second modes.

Preprints.org (www.preprints.org) | NOT PEER-REVIEWED | Posted: 2 June 2023 doi:10.20944/preprints202306.0155.v1

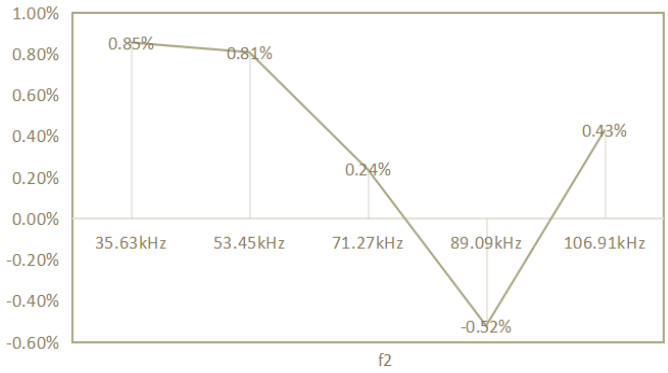

Figure 11. Effect of high frequency of USJ on second mode maximum growth rate.

3.1.3. Effects of Amplitude Control

One-way ANOVA is performed for the first mode growth rates as the frequency changes, which are controlled by the amplitude of USJ, as shown in Figure 12. It can be seen that when a=0.001 and 0.003, the growth rate of the first mode is greater than that of the uncontrolled case, which plays a role in promoting transition, while when a=0.005, 0.007, 0.009, it plays a suppressing role. When a=0.009, the suppression effect is the best.

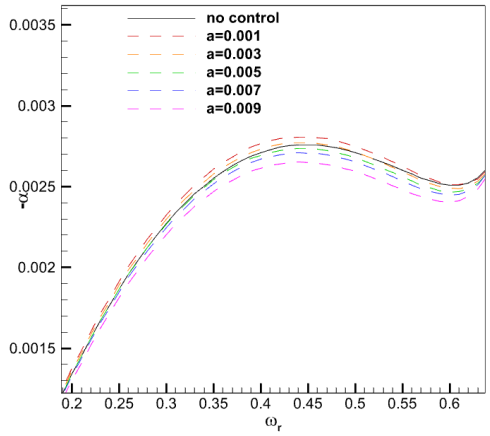

Figure 12. The first mode growth rate varies with frequency, controlled by the amplitude of USJ.

The percentage of difference between the maximum growth rate of the first mode and the uncontrolled case is used to make a line plot with the amplitude level, as shown in Figure 13. It can be seen that with the increase of amplitude, the control effect on transition gradually changes from promotion to suppression, and the higher the amplitude, the better the suppression effect, reaching -3.99% when a=0.009. The control effect of amplitude on transition is between low frequency f_1 and high frequency f_2.

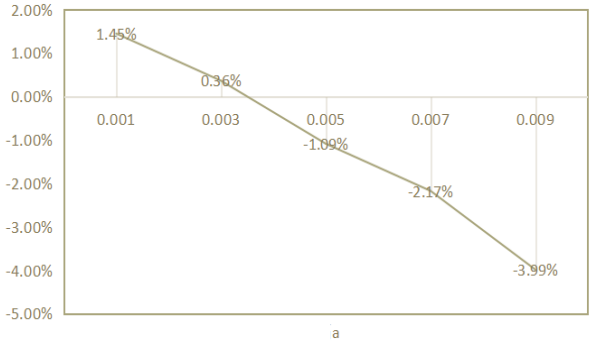

Figure 13. Effect of amplitude of USJ on first mode maximum growth rate.

Preprints.org (www.preprints.org) | NOT PEER-REVIEWED | Posted: 2 June 2023 doi:10.20944/preprints202306.0155.v1

One-way ANOVA is performed for the second mode growth rates as the frequency changes, which are controlled by the amplitude of USJ, as shown in Figure 14. It can be seen that when *a*=0.001, 0.003, 0.005, 0.007 the growth rate of the second mode is greater than that of the uncontrolled case, which plays a promoting role in transition, while when *a*=0.009 plays a suppressing role.

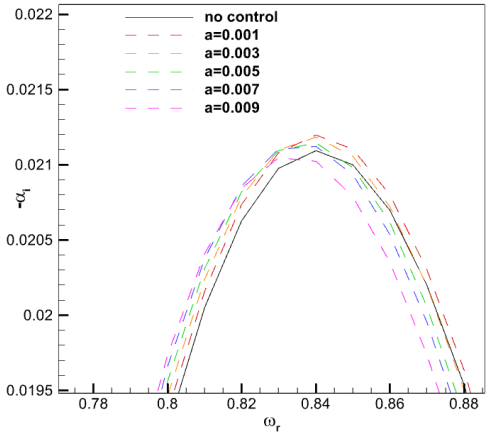

Figure 14. The second mode growth rate varies with frequency, controlled by the amplitude of USJ.

The percentage of difference between the maximum growth rate of the second mode and the uncontrolled case is used to make a line plot with the amplitude level, as shown in Figure 15. It can be seen that with the increase of *a*, the control effect on the second mode gradually changes from promotion to suppression, and the value reaches -0.24% when *a*=0.009.

To sum up, in order to achieve the suppression effect on the first and second modes, *a* should be 0.009.

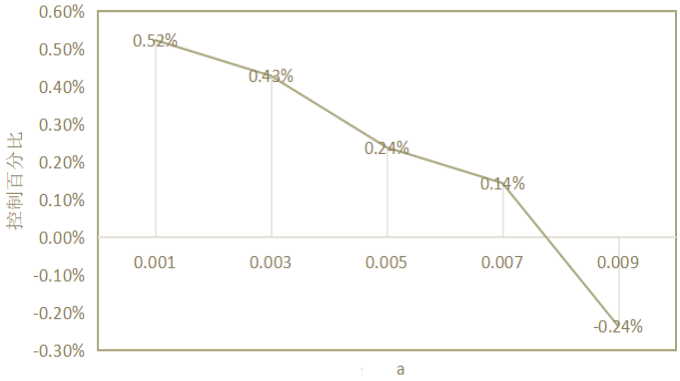

Figure 15. Effect of amplitude of USJ on second mode maximum growth rate.

3.2. Results of Synthetic Jet Arranged Downstream of Synchronization Point

The maximum growth rate of the first mode and the second mode of each case is shown in the second and third columns of Table 6, with synthetic jet is arranged downstream of the synchronization point. The fourth and fifth columns are the percentage of promotion or suppression relative to the first and second modes in the uncontrolled case, with positive values indicating promotion and negative values indicating suppression. It can be seen that DSJ plays a role in promoting transition, more obvious on the first mode.

Table 6. Test results of each case of DSJ.

Case	mode-1	mode-2	mode-1*	mode-2*
1	0.00280	0.02117	1.45%	0.43%

Preprints.org (www.preprints.org) | NOT PEER-REVIEWED | Posted: 2 June 2023 doi:10.20944/preprints202306.0155.v1

2	0.00291	0.02121	5.43%	0.62%
3	0.00287	0.02120	3.99%	0.57%
4	0.00329	0.02128	19.22%	0.95%
5	0.00301	0.02158	9.04%	2.36%
6	0.00290	0.02123	5.15%	0.72%
7	0.00280	0.02117	1.60%	0.43%
8	0.00302	0.02128	9.52%	0.95%
9	0.00308	0.02122	11.52%	0.68%
10	0.00285	0.02126	3.37%	0.85%
11	0.00285	0.02120	3.23%	0.55%
12	0.00301	0.02131	8.94%	1.10%
13	0.00297	0.02128	7.67%	0.94%
14	0.00287	0.02119	4.08%	0.51%
15	0.00311	0.02172	12.72%	3.03%
16	0.00297	0.02128	7.53%	0.94%
17	0.00292	0.02124	5.74%	0.78%
18	0.00283	0.02118	2.54%	0.47%
19	0.00321	0.02124	16.46%	0.77%
20	0.00297	0.02145	7.49%	1.77%
21	0.00291	0.02124	5.29%	0.77%
22	0.00283	0.02119	2.55%	0.51%
23	0.00302	0.02129	9.54%	1.01%
24	0.00298	0.02120	7.95%	0.56%
25	0.00320	0.02185	16.01%	3.67%

Case 4 has the strongest promotion effect on the first mode, reaching nearly 20%, and case 25 has the strongest promotion effect on the second mode, also reaching 3.67%, which is shown in Figure 16 below.

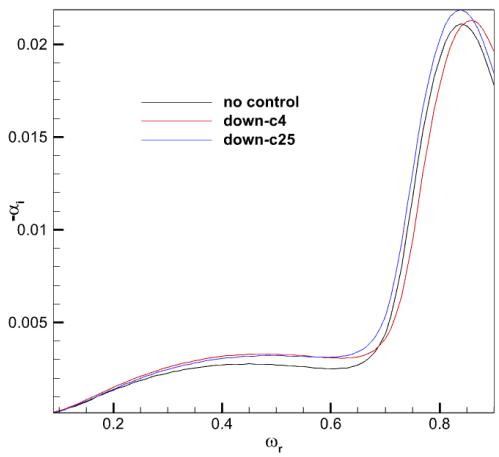

Figure 16. Growth rate varies with frequency in cases 4 and 25 of DSJ.

Preprints.org (www.preprints.org) | NOT PEER-REVIEWED | Posted: 2 June 2023 doi:10.20944/preprints202306.0155.v1

The multi-factor variance analysis of the control effect of the DSJ on the first mode shows that f_2 and a have a significant difference relationship on the first mode, while f_1 has a small difference relationship on the first mode, as shown in Table 7.

Table 7. Results of multivariate variance analysis of the first mode of the DSJ.

Source of variance	Sum of squares	df	Mean square	F	p
Intercept	0.141	1	0.141	395.066	0.0002
f_1	0.001	4	0.000	0.897	0.496
f_2	0.020	4	0.005	14.265	0.0001
a	0.028	4	0.007	19.928	0.0003
Residual	0.004	12	0.000		

The control effect of the DSJ on the second mode is analyzed by multi-factor variance. The results show that f_2 and a have a significant difference relation to the second mode, while f_1 has a small difference relation to the second mode, as shown in Table 8.

Table 8. Results of multi-factor variance analysis of the second mode of the DSJ.

Source of variance	Sum of squares	df	Mean square	F	p
Intercept	0.003	1	0.003	185.392	0.0003
f_1	0.000	4	0.000	1.868	0.181
f_2	0.001	4	0.000	18.457	0.0002
a	0.000	4	0.000	5.067	0.013
Residual	0.000	12	0.000		

3.2.1. Effects of Low Frequency Control

One-way ANOVA is performed for the first mode growth rates as the frequency changes, which are controlled by the low frequency of DSJ, as shown in Figure 17. It can be seen that under the five levels of f_1, the growth rate of the first mode is greater than that of the uncontrolled case, and transition is promoted. When f_1=7.12kHz, the promotion effect is the weakest, and when f_1=17.82kHz, the promotion effect is the strongest.

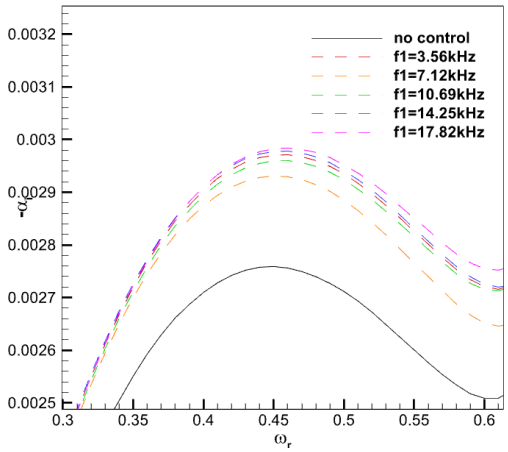

Figure 17. the first mode growth rate varies with frequency, controlled by the low frequency of DSJ.

Preprints.org (www.preprints.org) | NOT PEER-REVIEWED | Posted: 2 June 2023 doi:10.20944/preprints202306.0155.v1

The percentage of difference between the maximum growth rate of the first mode and the uncontrolled case is used to make a line plot with the low frequency level, as shown in Figure 18. It can be seen that the promotion effect is the weakest when f_1=7.12kHz, and there is little difference in the promotion effect in other cases.

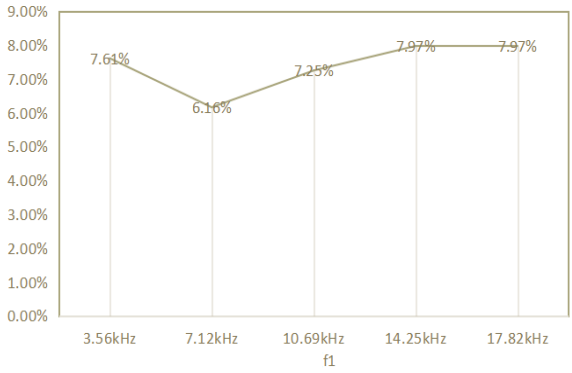

Figure 18. Effect of low frequency of DSJ on first mode maximum growth rate.

One-way ANOVA is performed for the second mode growth rates as the frequency changes, which are controlled by the low frequency of DSJ, as shown in Figure 19. It can be seen that under the five levels of f_1, the growth rate of the second mode is greater than that of the uncontrolled case, and transition is promoted. When f_1=7.12kHz, the promotion effect is the weakest.

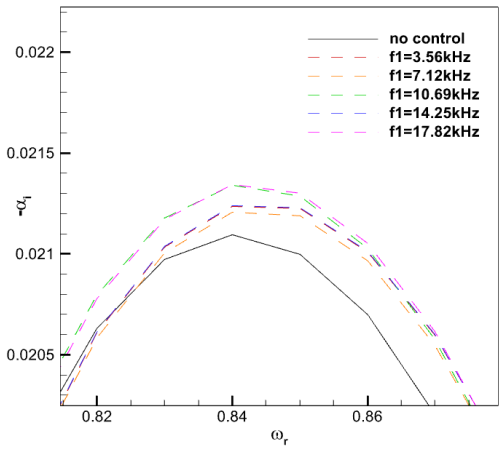

Figure 19. Variation of the second mode growth rate with frequency under the control of low frequency DSJ.

The percentage of difference between the maximum growth rate of the second mode and the uncontrolled case is used to make a line plot with the low frequency level, as shown in Figure 20. It can be seen that there is little difference in the control of the second mode by each level of f_1, all of which are about 1%. When f_1=7.12kHz, the promotion effect is the weakest, which is 0.52%.

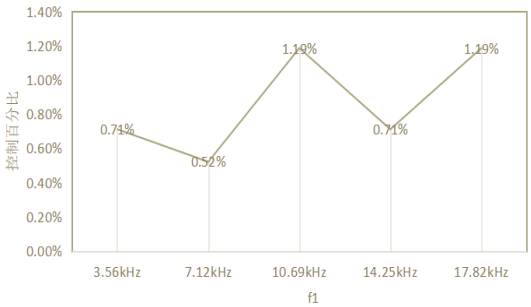

Figure 20. Effect of low frequency of DSJ on second mode maximum growth rate.

Preprints.org (www.preprints.org) | NOT PEER-REVIEWED | Posted: 2 June 2023 doi:10.20944/preprints202306.0155.v1

3.2.2. Effects of High Frequency Control

One-way ANOVA is performed for the first mode growth rates as the frequency changes, which are controlled by the high frequency of DSJ, as shown in Figure 21. It can be seen that under the five levels of f_2, the growth rate of the first mode is greater than that of the uncontrolled case, and transition is promoted. When f_2=89.09kHz, the promotion effect is strongest, and when f_2=35.63kHz, the promotion effect is weakest.

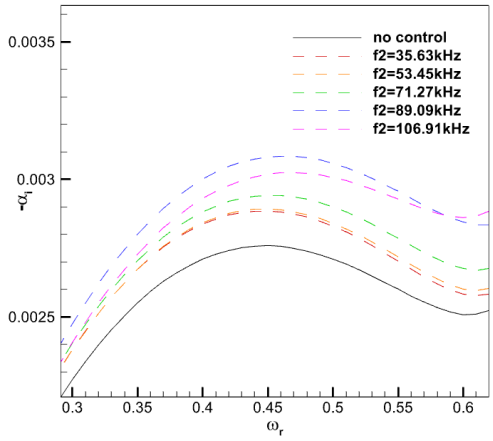

Figure 21. The first mode growth rate varies with frequency, controlled by the high frequency of DSJ.

The percentage of difference between the maximum growth rate of the first mode and the uncontrolled case is used to make a line plot with the high frequency level, as shown in Figure 22 below. It can be seen that with the increase of f_2, the effect of transition promotion becomes more and more obvious, reaching a peak value of 11.59% when f_2=89.09kHz, and then slightly decreasing. Compared with low frequency f_1. The control effect of high frequency f_2 is more obvious.

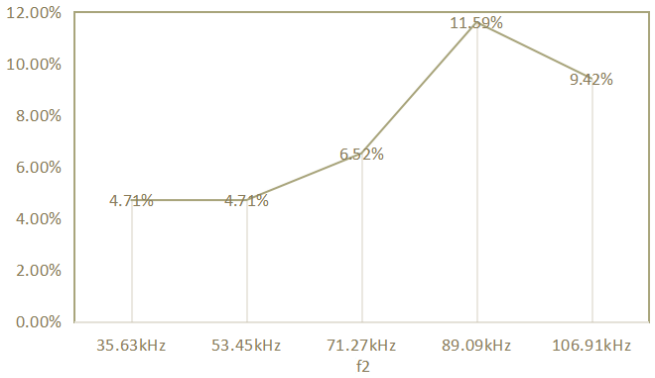

Figure 22. Effect of high frequency of DSJ on first mode maximum growth rate.

One-way ANOVA is performed for the second mode growth rates as the frequency changes, which are controlled by the high frequency of DSJ, as shown in Figure 23. It can be seen that at the five levels of f_2, the growth rate of the second mode is greater than that of the uncontrolled case, and transition is promoted, among which the promotion effect is the most obvious when f_2=106.91kHz. When f_2=89.09kHz, the frequency corresponding to the maximum growth rate of the second mode increases slightly compared with other levels and the uncontrolled case; when f_2=106.91kHz, the frequency corresponding to the maximum growth rate of the second mode decreases slightly compared with other levels.

Preprints.org (www.preprints.org) | NOT PEER-REVIEWED | Posted: 2 June 2023 doi:10.20944/preprints202306.0155.v1

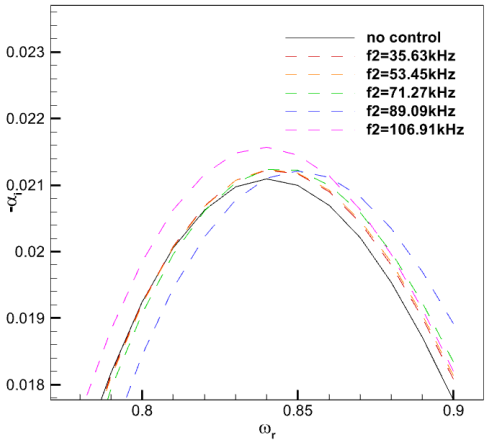

Figure 23. The second mode growth rate varies with frequency, controlled by the high frequency of DSJ.

The percentage of difference between the maximum growth rate of the second mode and the uncontrolled case is used to make a line plot with the high frequency level, as shown in Figure 24. It can be seen that at the lower frequency (f_2=35.63kHz, 53.45kHz, 71.27kHz, 89.09kHz), the weaker promotion effect, with an effect of 0.5%. However, when f_2=106.91kHz, the promotion effect is increased to 2.28%. It can be seen that the high frequency control of the DSJ has a strong effect on promoting transition when the frequency reaches about 100kHz.

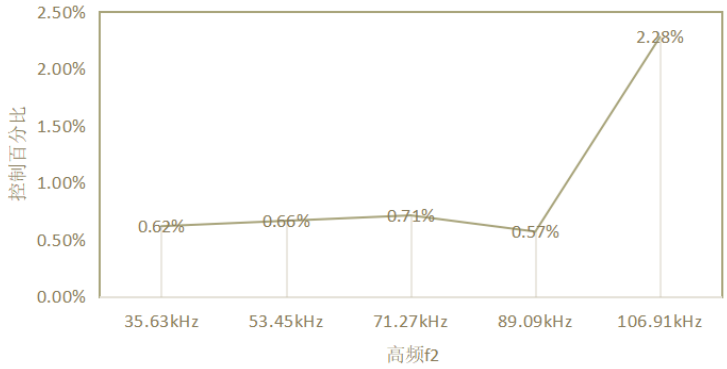

Figure 24. Effect of high frequency of DSJ on maximum growth rate of second mode.

3.2.3. Effects of Amplitude Control

One-way ANOVA is performed for the first mode growth rates as the frequency changes, which are controlled by the amplitude of DSJ, as shown in Figure 25. It can be seen that under the five levels of amplitude, the growth rate of the first mode is greater than that of the uncontrolled case, and transition is promoted.

Preprints.org (www.preprints.org) | NOT PEER-REVIEWED | Posted: 2 June 2023 doi:10.20944/preprints202306.0155.v1

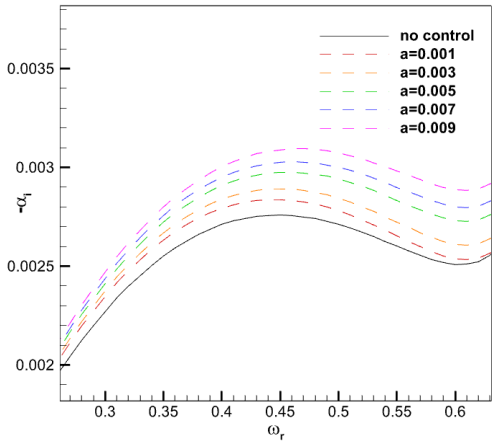

Figure 25. The first mode growth rate varies with frequency, controlled by the amplitude of DSJ.

The percentage of difference between the maximum growth rate of the first mode and the uncontrolled case is used to make a line plot with the amplitude level, as shown in Figure 26. It can be seen that with the increase of amplitude, the promoting effect on the first mode becomes more and more strong, reaching 11.96% when a=0.009.

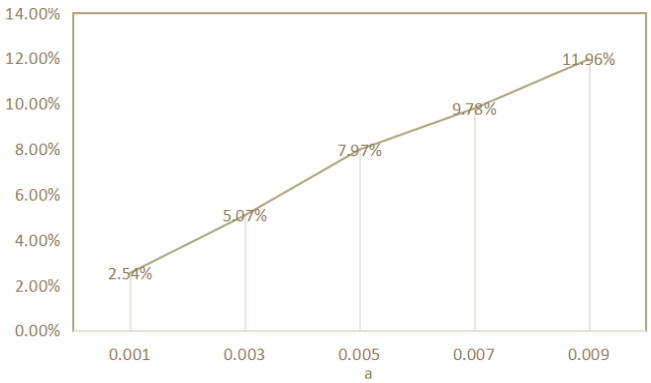

Figure 26. Effect of amplitude of DSJ on first mode maximum growth rate.

One-way ANOVA is performed for the second mode growth rates as the frequency changes, which are controlled by the amplitude of DSJ, as shown in Figure 27. It can be seen that at the five levels of amplitude, the growth rate of the second mode is greater than that of the uncontrolled case, and transition is promoted, and the frequency corresponding to the maximum growth rate of the second mode at the five levels slightly increases compared with the uncontrolled case.

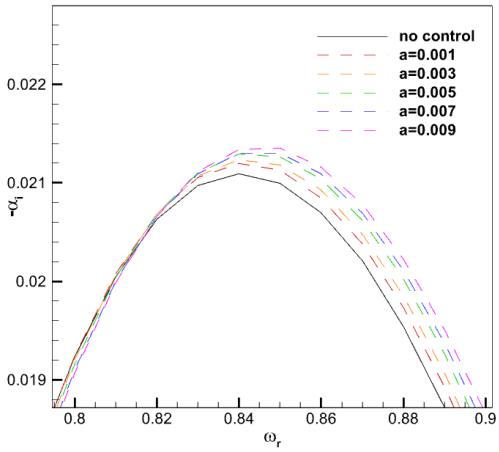

Figure 27. The second mode growth rate varies with frequency, controlled by the amplitude of DSJ.

Preprints.org (www.preprints.org) | NOT PEER-REVIEWED | Posted: 2 June 2023 doi:10.20944/preprints202306.0155.v1

The percentage of difference between the maximum growth rate of the second mode and the uncontrolled case is used to make a line plot with the amplitude level, as shown in Figure 28. It can be seen that with the increase of amplitude, the promotion effect on second mode becomes more and more strong, reaching 1.19% when a = 0.009. It can be seen that under the condition that the jet is arranged in the downstream, the amplitude has an obvious positive correlation with transition promotion for both first mode and second mode.

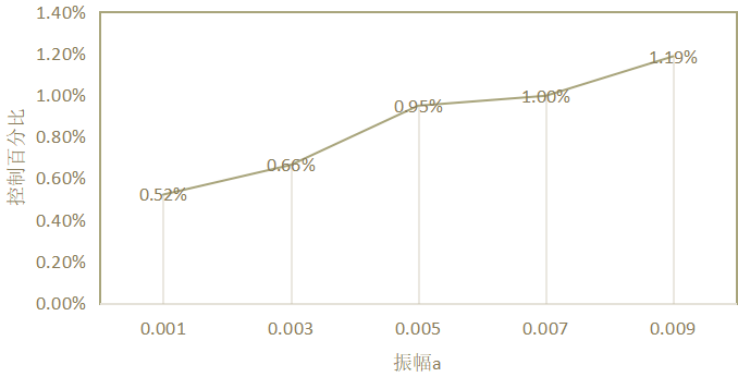

Figure 28. Effect of amplitude a of the DSJ on the maximum growth rate of the second mode.

4. Variation of Growth Rate with Spanwise Wave Number

In the variation of growth rate with frequency in the previous section, the spanwise wave number is fixed at β_r=0, so it is impossible to know the rule of growth rate varies with spanwise wave number. In this section, the change of the growth rate with the spanwise wave number in the first mode (ω=0.45) and second mode (ω=0.84) will be studied.

Figure 29 shows the change of the first mode growth rate with spanwise wave number β_r in the uncontrolled case. It can be seen that with the increase of the spanwise wave number, the growth rate gradually increases and reaches the peak value at about 0.0062, where β_r=0.6. When β_r=1.2 and the growth rate $-\alpha_i$<0, the disturbance decreases and the flow tends to be stable.

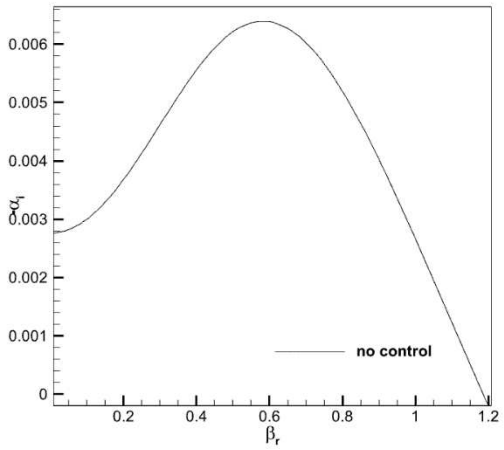

Figure 29. First mode growth rate varies with the spanwise wave number in the uncontrolled case.

Figure 30 shows the change of the second mode growth rate of with the spanwise wave number β_r in the uncontrolled case. It can be seen that with the increase of the spanwise wave number, the growth rate gradually decreases, and when β_r=1, the growth rate is less than zero, the disturbance decreases and the flow tends to be stable.

Preprints.org (www.preprints.org) | NOT PEER-REVIEWED | Posted: 2 June 2023 doi:10.20944/preprints202306.0155.v1

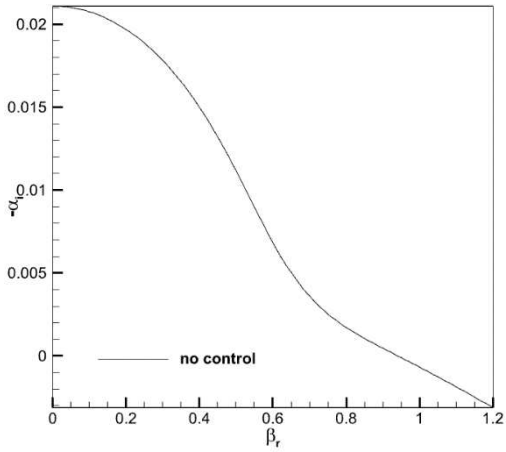

Figure 30. Second mode growth rate varies with the spanwise wave number in the uncontrolled case.

4.1. Results of Synthetic Jet Arranged Upstream of Synchronization Point

4.1.1. Effects of Low Frequency Control

Figure 31 shows the one-way ANOVA performed for the first mode growth rates as the spanwise wave number changes, which are controlled by the low frequency of USJ. It can be seen that when β_r=0, only f_1=14.25kHz is to promote transition, other levels are to suppress transition, and with the increase of β_r, f_1=7.12kHz, 10.69kHz, 14.25kHz are to promote transition, only f_1=3.56kHz, 17.82kHz is to suppress transition. It can be seen that if the effect of transition suppression is to be achieved under the condition of all spanwise wave number, the low frequency f_1 should be 3.56kHz and 17.82kHz.

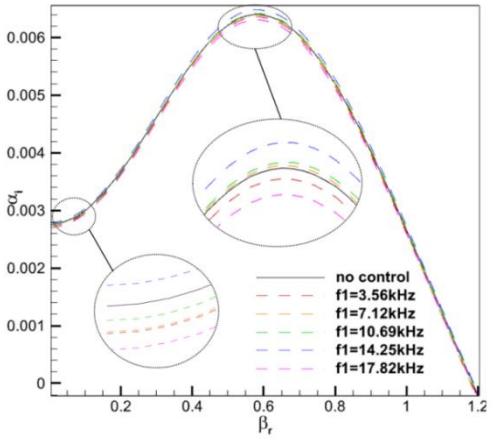

Figure 31. The first mode growth rate varies with spanwise wave number, controlled by the low frequency of USJ.

Figure 32 shows the one-way ANOVA performed for the second mode growth rates as the spanwise wave number changes, which are controlled by the low frequency of USJ. It can be seen that when β_r=0, f_1=17.82kHz is to suppress transition, other levels are to promote transition, and with the increase of βr, when β_r=0.5, the five levels of f_1 turn to promote transition, and when β_r=0.8, f_1=7.12kHz turns to suppress transition. It can be seen that the control effect of low frequency f_1 on the second mode will change with the change of the spanwise wave number, and no low frequency can cause the suppression effect on the second mode in all spanwise wave number.

Preprints.org (www.preprints.org) | NOT PEER-REVIEWED | Posted: 2 June 2023 doi:10.20944/preprints202306.0155.v1

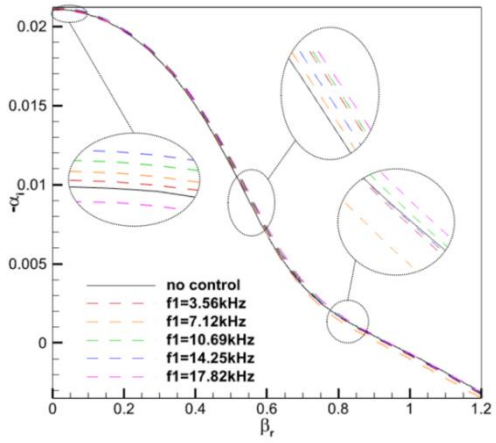

Figure 32. The second mode growth rate varies with spanwise wave number, controlled by the low frequency of USJ.

4.1.2. Effects of High Frequency Control

Figure 33 shows the one-way ANOVA performed for the first mode growth rates as the spanwise wave number changes, which are controlled by the high frequency of USJ. It can be seen that when β_r=0, f_2=71.27kHz, 89.09kHz and 106.91kHz have suppressing effects on transition, while with the increase of β_r, the control effect of f_2=71.27kHz decreases, while the control effect of other levels remains unchanged. It can be seen that in order to achieve the effect of transition suppression under the condition of full spanwise wave number, the high frequency f_2 should be 89.09kHz and 106.91kHz.

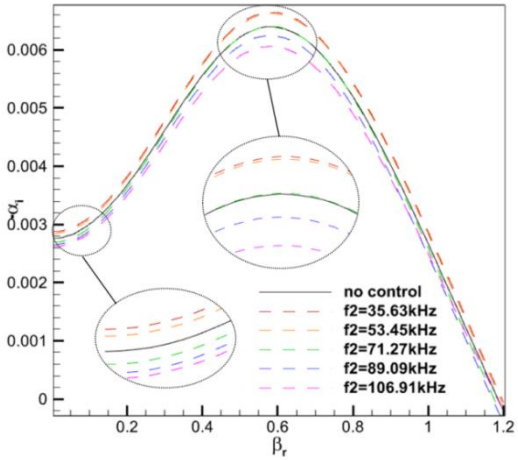

Figure 33. The first mode growth rate varies with spanwise wave number, controlled by the high frequency of USJ.

Figure 34 shows the one-way ANOVA performed for the second mode growth rates as the spanwise wave number changes, which are controlled by the high frequency of USJ. It can be seen that when β_r=0, f_2=89.09kHz, 106.91kHz plays a suppressing role on transition, and with increase of βr, when β_r=0.8, f_2=106.91kHz turns to promotion effect, and the other levels turn to suppression effect. It can be seen that the high frequency control with low frequency will show suppression effect under the condition of high spanwise wave number. In order to achieve the suppression effect of the second mode under the condition of all spanwise wave number, high frequency should be 89.09kHz.

Preprints.org (www.preprints.org) | NOT PEER-REVIEWED | Posted: 2 June 2023 doi:10.20944/preprints202306.0155.v1

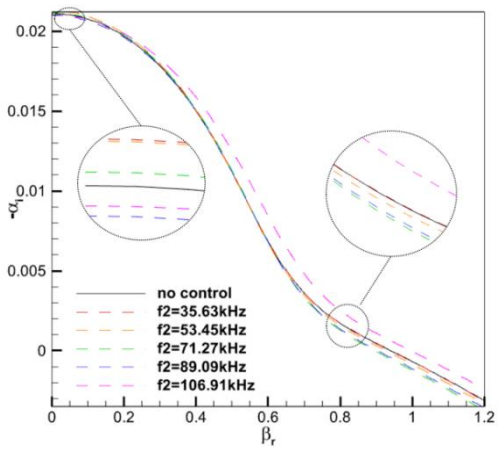

Figure 34. The second mode growth rate varies with spanwise wave number, controlled by the high frequency of USJ.

4.1.3. Effects of Amplitude Control

Figure 35 shows the one-way ANOVA performed for the first mode growth rates as the spanwise wave number changes, which are controlled by the amplitude of USJ. It can be seen that a=0.001 and 0.003 play a role in promoting transition, and a=0.005, 0.007, 0.009 play a suppressing effect when β_i=0, and as the increase of β_r, a=0.005 becomes almost no control effect, the growth rate curve and the uncontrolled case basically coincide, the control effect of the rest level is unchanged. It can be seen that if you want to achieve the effect of transition suppression in the case of all spanwise wave number, amplitude should be 0.007 and 0.009.

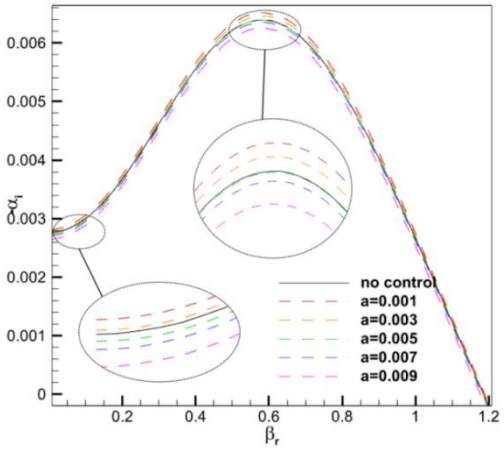

Figure 35. The first mode growth rate varies with spanwise wave number, controlled by the amplitude of USJ.

Figure 36 shows the one-way ANOVA performed for the second mode growth rates as the spanwise wave number changes, which are controlled by the amplitude of USJ. It can be seen that only a=0.009 has a suppressing effect on transition when β_i=0, and with the increase of β_r, the five levels of amplitude turn to promote transition when β_i=0.5, the five levels of a turn to suppress transition when β_i=0.8.

Preprints.org (www.preprints.org) | NOT PEER-REVIEWED | Posted: 2 June 2023 doi:10.20944/preprints202306.0155.v1

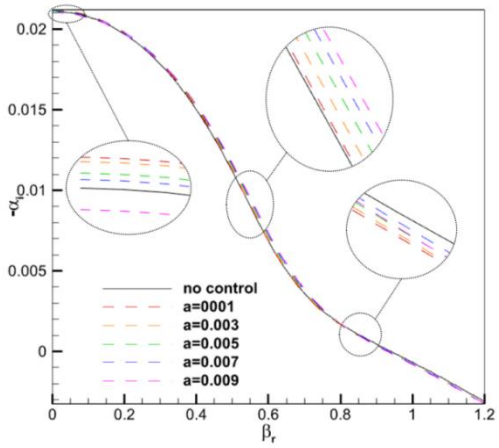

Figure 36. The second mode growth rate varies with spanwise wave number, controlled by the amplitude of USJ.

4.2. Results of Synthetic Jet Arranged Downstream of Synchronization Point

4.2.1. Effects of Low Frequency Control

Figure 37 shows the one-way ANOVA performed for the first mode growth rates as the spanwise wave number changes, which are controlled by the low frequency of DSJ. It can be seen that the control rule of low frequency is the same under each spanwise wave number.

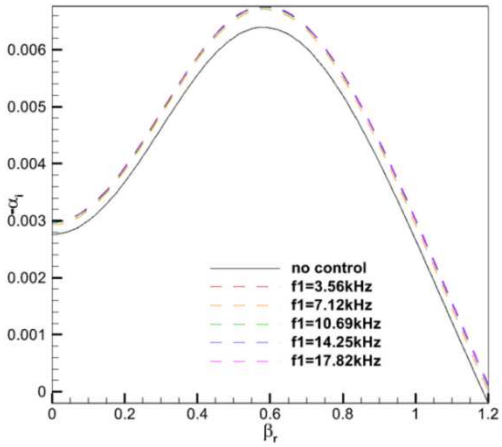

Figure 37. The first mode growth rate varies with spanwise wave number, controlled by the low frequency of DSJ.

Figure 38 shows the one-way ANOVA performed for the second mode growth rates as the spanwise wave number changes, which are controlled by the low frequency of DSJ. When β_r=0, the five levels of f_1 all turn to promote transition, but with the increase of β_r, when β_r=0.5, only f_1=17.82kHz is to promote transition, and the other four levels all play a suppressing role on transition, when β_r=0.8, all levels turn to promote transition. It can be seen that low frequency of the jet arranged in the downstream promotes transition to the second mode growth rate at low and high spanwise wave numbers, while at medium spanwise wave numbers, transition is suppressed.

Preprints.org (www.preprints.org) | NOT PEER-REVIEWED | Posted: 2 June 2023 doi:10.20944/preprints202306.0155.v1

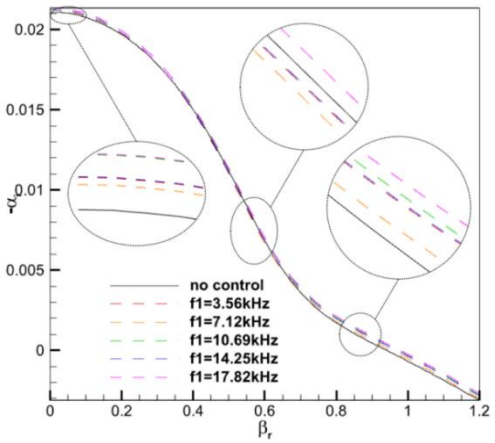

Figure 38. The second mode growth rate varies with spanwise wave number, controlled by the low frequency of DSJ.

4.2.2. Effects of High Frequency Control

Figure 39 shows the one-way ANOVA performed for the first mode growth rates as the spanwise wave number changes, which are controlled by the high frequency of DSJ. It can be seen that the control rule of low frequency is the same under each spanwise wave number.

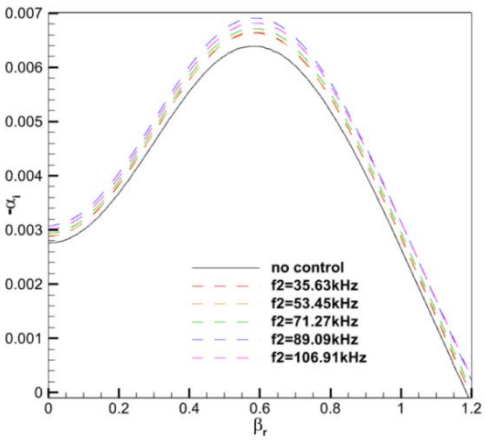

Figure 39. The first mode growth rate varies with spanwise wave number, controlled by the high frequency of DSJ.

Figure 40 shows the one-way ANOVA performed for the second mode growth rates as the spanwise wave number changes, which are controlled by the high frequency of DSJ. It can be seen that all the five levels of f_2 turn to promote transition when β_r=0, and as β_r increases, only f_2=106.91kHz promote transition when β_r=0.5, the other four levels are used to suppress transition. When βr=0.8, all the levels turn to promote transition again. It can be seen that the high frequency f_2 of the jet arranged in the downstream promotes transition for the second mode growth rate at low and high propagation wave numbers, while at medium spanwise wave numbers, transition is restrained. This is similar to the control rule of low frequency.

Preprints.org (www.preprints.org) | NOT PEER-REVIEWED | Posted: 2 June 2023 doi:10.20944/preprints202306.0155.v1

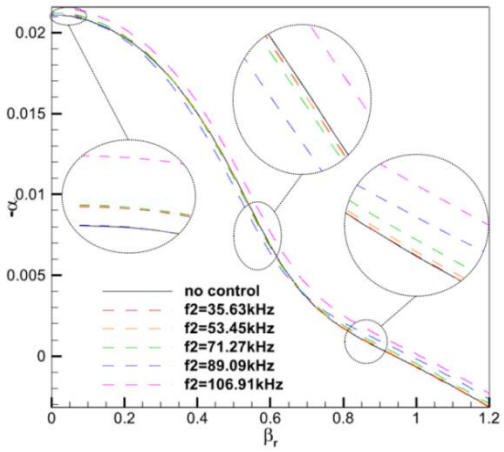

Figure 40. The second mode growth rate varies with spanwise wave number, controlled by the high frequency of DSJ.

4.2.3. Effects of Amplitude Control

Figure 41 shows the one-way ANOVA performed for the first mode growth rates as the spanwise wave number changes, which are controlled by the amplitude of DSJ. The control rule of amplitude is the same under each spanwise wave number.

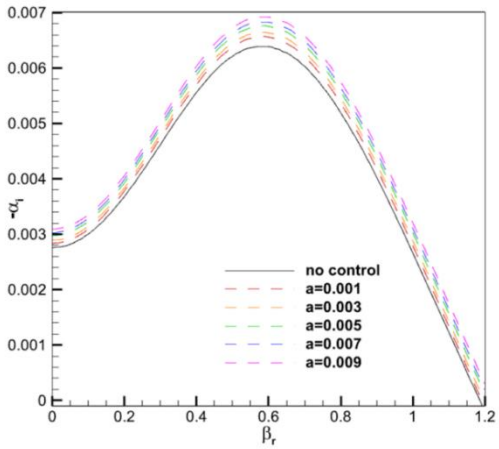

Figure 41. The first mode growth rate varies with spanwise wave number, controlled by the amplitude of DSJ.

The Figure 42 shows the one-way ANOVA performed for the second mode growth rates as the spanwise wave number changes, which are controlled by the amplitude of DSJ. It can be seen that when β_r=0 the five levels of amplitude play a promote role to transition, and with the increase of β_r=0.8, five levels are very weak on the transition control effect when β_r=0.5. when β_r=0.8, only a=0.001 suppresses transition, the remaining four levels turn to promote transition. It can be seen that the amplitude of the jet arranged in the downstream promotes transition at second mode growth rate under low and high spanning wave numbers. Only a=0.001 has a weak restraining effect on transition under high spanning wave numbers.

Preprints.org (www.preprints.org) | NOT PEER-REVIEWED | Posted: 2 June 2023 doi:10.20944/preprints202306.0155.v1

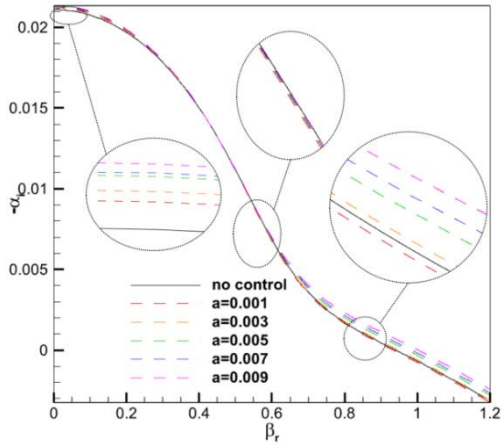

Figure 42. The second mode growth rate varies with spanwise wave number, controlled by the amplitude of DSJ.

5. Flow Field Structure Analysis

Figure 43 shows the pressure pulsation diagram of the uncontrolled flow field. It can be seen that the twin lattice structure grows and tends to become more unstable in the downstream, where the boundary layer gradually becomes unstable and turns to turbulence.

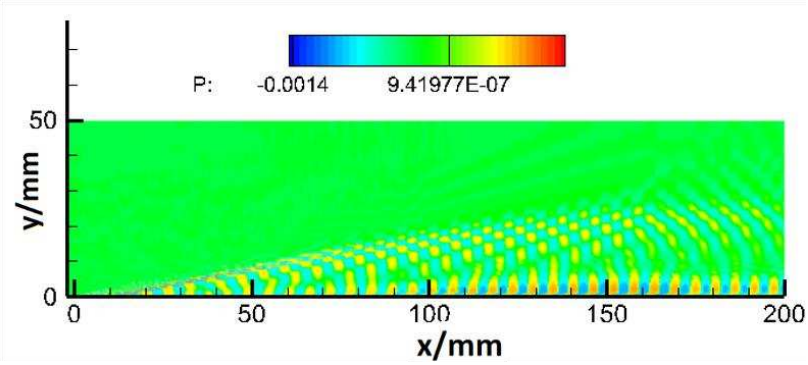

Figure 43. Pressure pulsation diagram in uncontrolled state.

Figure 44 shows the pressure pulsation diagram of the flow field with transition suppressed, which is the fourth case of jet arranged upstream, with f_1=3.56kHz, f_2=89.9kHz and a=0.009. Due to the variation of pressure fluctuations over time, it is not convenient to conduct one-way ANOVA, so only typical experimental groups are selected for analysis. It can be seen that the bi-frequency synthetic jet forms weak expansion and compression waves upstream, while after the wave system, the twin lattice structure of pressure pulsation is relatively small compared to the uncontrolled state, the flow tends to stabilize and the transition is suppressed.

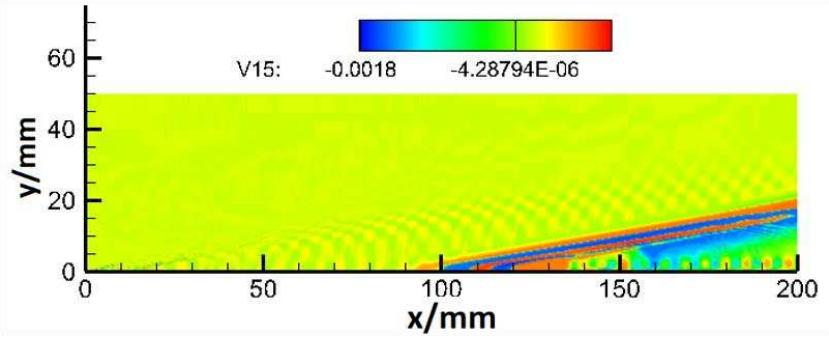

Figure 44. Pressure pulsation diagram with transition suppressed.

 doi:10.20944/preprints202306.0155.v1

Figure 45 shows the pressure pulsation diagram of the flow field with transition promoted, which is the 19th group of actuators arranged downstream. It can be seen that after the wave system, the twin lattice structure of pressure pulsation increases even more until it merges with the wave system structure. The pulsation outside the wave system is more obvious compared to the uncontrolled state, and the flow tends to be unstable, promoting transition.

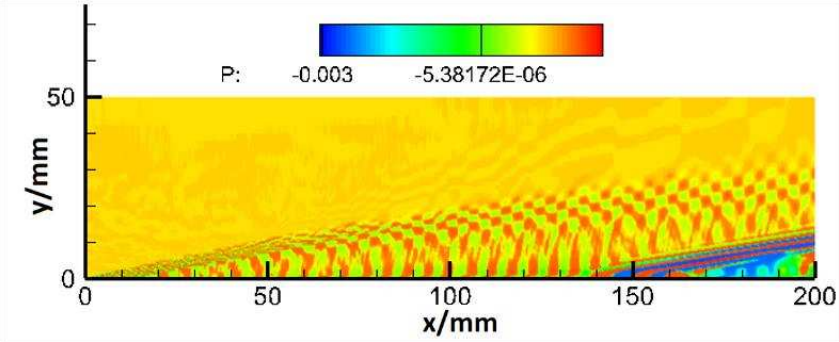

Figure 45. Pressure pulsation diagram with transition promoted.

Overall, the bi-frequency synthetic jet reduces the pressure pulsation in the flow field during transition suppression, weakens the twin lattice structure of pressure pulsation, and thus improves the stability of the flow.

6. Conclusions

This paper proposes a novel transition delaying control method of hypersonic boundary layer transition based on bi-frequency synthetic jet. Orthogonal table and multi-factor/one-way ANOVA are used to study the control effect of the three parameters of the bi-frequency synthetic jet located in the upstream and downstream of the synchronization point: low frequency, high frequency and amplitude on the growth rate of unstable modes, which are reflected in the change of the growth rate with frequency and the change of the growth rate with the spanwise wave number. Linear stability theory is adopted to analyze the control effect.

In terms of the change of growth rate with frequency, the results of multi-factor variance analysis show that, for the USJ, the influence of high frequency on the unstable mode is greater, while the influence of amplitude and low frequency is less. For the DSJ, the high frequency and amplitude have greater influence on the unstable mode, while the low frequency has less influence. One-way ANOVA of the three factors shows that, for the jet arranged in the upstream, the four levels in the low frequency can have a small suppressing effect on the first mode, but a weak control effect on the second mode; The higher the high frequency, the stronger the suppressing effect on the first mode, while for the second mode only produces a small suppression effect at f_2=89.09kHz; The larger the amplitude, the weaker the promoting effect for the first mode and the second mode, and the more obvious the suppressing effect. For the jet arranged in the downstream, all levels of the three parameters have a promoting effect on first mode and second mode. The five levels of low frequency have little difference in control effect. The higher high frequency, the more obvious the promotion effect. The higher the amplitude, the more obvious the promotion effect.

As for the change of the growth rate with the spanwise wave number, one-way ANOVA was carried out for the three influencing factors respectively. The results show that, for the jet arranged in the upstream, the control rule of the low frequency is: for the first mode, some of the levels that produce suppressing effect under the low spanwise wave number show weak promotion effect on the medium spanwise wave number (i.e., when the growth rate peaks); for the second mode, all the levels show promotion effect under the medium spanwise wave number, some levels show suppressing effect at high spanwise wave number; The control rule of high frequency is as follows: for the first mode, only f_2=89.09kHz and 106.91kHz can achieve the effect of transition suppression at all spanwise wave number; for the second mode, part of levels present the promotion effect at low

 doi:10.20944/preprints202306.0155.v1

spanwise wave number while the suppression effect at high spanwise wave number. Thus: for the first mode, the control rule is consistent under the all spanwise wave number; for the second mode, the promoting effect appears at all levels under the middle spanwise wave number, and the suppressing effect appears at all levels under the high spanwise wave number. For the synthetic jet arranged in the downstream, the control rules of the three influencing factors are as follows: for the first mode, the control rules are the same; for the second mode, all the levels present a promoting effect under the low spanwise wave number, a suppressing effect under the medium spanwise wave number, and a promoting effect under the high spanwise wave number. Only a=0.001 shows suppressing effect under high spanwise wave number.

Based on the above rules, the three influencing factors and the location of the synthetic jet should be selected as f_1=3.56kHz, f_2=89.9kHz, a=0.009, and arranged upstream to obtain the optimal suppression effect, with the maximum growth rate of the first mode is reduced by 9.06% and that of the second mode is reduced by 1.28% compared with the uncontrolled state. Observing from the pressure pulsation graph, it weakens the twin lattice structure of pressure pulsation, and thus improves the stability of the flow.

Data Availability Statement: The data that support the findings of this study are available from the corresponding author upon reasonable request.

Acknowledgement: This work is funded by the National Natural Science Foundation of China (grants: 12202488, 12002377), Natural Science Program of National University of Defense Technology (ZK22-30) and Independent Cultivation Project for Young Talents in College of Aerospace Science and Engineering. Supercomputer time provided by the National Supercomputing Center in Beijing is also gratefully acknowledged.

Author Declarations Section: The authors have no conflicts to declare.

References

1. Liu Qiang, Luo Zhenbing, Wang Lin, Tu Guohua, Deng, Xiong, and Zhou Yan. Direct numerical simulations of supersonic turbulent boundary layer with streamwise-striped wall blowing [J]. Aerospace Science and Technology, 2021, 110, 106510.
2. Fedorov A. Transition and stability of high-speed boundary layers [J]. Annual Review of Fluid Mechanics, 2011, 43(1): 79-95
3. Kachanov Y.S. Physical mechanisms of laminar-boundary-layer transition [J]. Annual Review of Fluid Mechanics, 1994, 26(1): 411-482
4. Ma Yanbao, and Zhong Xiaolin. Receptivity of a supersonic boundary layer over a flat plate. Part 1. Wave structures and interaction [J]. Journal of Fluid Mechanics, 2003, 488: 31-78.
5. Craig S.A., Humble R.A., Hofferth J.W., and Saric W.S. Nonlinear behavior of the Mack mode in a hypersonic boundary layer [J]. Journal of Fluid Mechanics, 2019, 872: 74-99.
6. Zhong Xiaolin, and Wang Xiaowen. Direct numerical simulation on the receptivity, instability, and transition of hypersonic boundary layers [J]. Annual Review of Fluid Mechanics, 2012, 44(1): 527-561.
7. Mack L M. Computational of the stability of the laminar compressible boundary layers [J]. Methods in Computational Physical,1965, 4: 247-299.
8. Zurigat Y.H., Nayfeh A.H., and Masad J.A. Effect of pressure gradient on the stability of compressible boundary layers [J]. AIAA Journal, 1992, 30(9): 2204-2211.
9. Malik M R. Prediction and control of transition in supersonic and hypersonic boundary layers [J]. AIAA Journal, 1989, 27(11): 1487-1493.
10. Kimmel R.L., and Poffie J. Effect of total temperature on boundary layer stability at Mach 6. [R]. Reston: AIAA1999-0816, 1999.
11. Paredes P., Choudhari M.M. and Li Fei. Transition delay via vortex generators in a hypersonic boundary layer at flight conditions [C]. 2018 Fluid Dynamics Conference, 2018.
12. Igarashi T., and Iida Y. Fluid flow and heat transfer around a circular cylinder with vortex generators [J]. Transactions of the Japan Society of Mechanical Engineers, Part B, 1985, 51(467): 2420-2427.
13. Schneider S.P. Effects of roughness on hypersonic boundary-layer transition [J]. Journal of Spacecraft and Rockets, 2008, 45(2): 193-209.
14. Fedorov A. Receptivity of hypersonic boundary layer to acoustic disturbances scattered by surface roughness [R]. Reston: AIAA-2003-3731, 2003.
15. Schneider S.P. Summary of hypersonic boundary-layer transition experiments on blunt bodies with roughness [J]. Journal of Spacecraft and Rockets, 2008, 45(6): 1090-1105

 doi:10.20944/preprints202306.0155.v1

16. Liu Xiaolin, Yi Shihe, Xu Xiwang, Shi Yang, Ouyang Tianci, and Xiong Haoxi. Experimental study of second-mode wave on a flared cone at Mach 6 [J]. Physics of Fluids, 2019, 31(7), 074108.
17. Fujii K. Experiment of the two-dimensional roughness effect on hypersonic boundary-layer transition [J]. Journal of Spacecraft and Rockets, 2006, 43(4): 731-738.
18. Gaponov S.A., and Terekhova N.M. Stability of supersonic boundary layer on a porous plate with a flexible coating [J]. Thermophysics and Aeromechanics, 2014, 21(2): 143-156
19. Morozov S.O., Lukashevich S.V., Soudakov V.G., and Shiplyuk A.N. Experimental study of the influence of small angles of attack and cone nose bluntness on the stabilization of hypersonic boundary layer with passive porous coating [J]. Thermophysics and Aeromechanics, 2018, 25(6): 793-800
20. Gaponov S.A., Ermolaev Y.G., Kosinov A.D., Lysenko V.I., Semenov N.V., and Smorodskii B.V. Influence of porous-coating thickness on the stability and transition of flat-plate supersonic boundary layer [J]. Thermophysics and Aeromechanics, 2012, 19(4): 555-560
21. Germain P D, Hornung H G. Transition on a slender cone in hypervelocity flow [J]. Experiments in Fluids, 1997, 22: 183-190.
22. Gaponov S.A., and Smorodsky B.V. Control of supersonic boundary layer and its stability by means of foreign gas injection through the porous wall [J]. International Journal of Theoretical and Applied Mechanics, 2016, 1: 97-103.
23. Miró F., and Pinna F. Injection-gas-composition effects on hypersonic boundary-layer transition [J]. Journal of Fluid Mechanics, 2020, 890, R4.
24. Orlik E., Fedioun I., and Lardjane N. Hypersonic boundary-layer transition forced by wall injection: a numerical study [J]. Journal of Spacecraft and Rockets, 2014, 51(4): 1306-1318
25. Liu Qiang, Luo Zhenbing, Deng Xiong, Yang Shengke, and Jiang Hao. Linear stability of supersonic boundary layer with synthetic cold/hot jet control [J]. Acta Physica Sinica, 2017, 66(23): 222-232.
26. Brett F.B., Paul M.D., Jennifer A.I., David W.A. and Scott A.B. PLIF visualization of active control of hypersonic boundary layers using blowing [R]. AIAA paper, 2008-4266, 2008.
27. Zhao Rui, Wen Chiyong, Tian Xudong, and Long Tiehan. Numerical simulation of local wall heating and cooling effect on the stability of a hypersonic boundary layer [J]. International Journal of Heat and Mass Transfer, 2018, 121: 986-998.
28. Unnikrishnan S., Gaitonde D.V. Instabilities and transition in cooled wall hypersonic boundary layers [J]. Journal of Fluid Mechanics, 2021, 915, A26.
29. Li Xinliang, Fu Dexun, Ma Yanwen, and Liang Xian. Direct numerical simulation of compressible turbulent flows [J]. Acta Mechanica Sinica, 2010, 26: 795-806.
30. Liu Qiang. Research on control methods and mechanisms of supersonic/hypersonic boundary layer drag reduction subject to active flow control [D]. Ph.D thesis of National University of Defense Technology, 2021.
31. Heisenberg W. Uber stabilitat und turbulenz von flussigkeits-stommen [J]. Annual Physics, 1924, 74: 577-627.